Annals of Botany **97**: 177–193, 2006
doi:10.1093/aob/mcj027, available online at www.aob.oxfordjournals.org

Floral Nectar Production and Nectary Anatomy and Ultrastructure of *Echinacea purpurea* (Asteraceae)

TYLER J. WIST and ARTHUR R. DAVIS*

Department of Biology, 112 Science Place, University of Saskatchewan, Saskatoon, SK, Canada S7N 5E2

Received: 7 August 2005 Returned for revision: 6 September 2005 Accepted: 25 October 2005 Published electronically: 9 December 2005

• *Background and Aims* In spite of the impressive species diversity in the Asteraceae and their widespread appeal to many generalist pollinators, floral-nectary ultrastructure in the family has rarely been investigated. To redress this, a study using *Echinacea purpurea*, a plant of horticultural and nutraceutical value, was undertaken. Nectar secretion of disc florets was compared with floral nectary ultrastructure taking into account nectar's potential impact upon the reproductive success of this outcrossing species.
• *Methods* Micropipette collections of nectar in conjunction with refractometry were used to determine the volume and nectar-sugar quantities of disc florets throughout their phenology, from commencement of its production to cessation of secretion. Light, scanning-electron and transmission-electron microscopy were utilized to examine morphology, anatomy and ultrastructure of nectaries of the disc florets.
• *Key Results* Florets were protandrous with nectar being secreted from anthesis until the third day of the pistillate phase. Nectar production per floret peaked on the first day of stigma receptivity, making the two innermost whorls of open florets most attractive to foraging visitors. Modified stomata were situated along the apical rim of the collar-like nectary, which surrounds the style base and sits on top of the inferior ovary. The floral nectary was supplied by phloem only, and both sieve elements and companion cells were found adjacent to the epidermis; the latter participated in the origin of some of the precursor cells that yielded these specialized cells of phloem. Companion cells possessed wall ingrowths (transfer cells). Lobed nuclei were a key feature of secretory parenchyma cells.
• *Conclusions* The abundance of mitochondria suggests an eccrine mechanism of secretion, although dictyosomal vesicles may contribute to a granulocrine process. Phloem sap evidently is the main contributor of nectar carbohydrates. From the sieve elements and companion cells, an apoplastic route via intercellular spaces and cell walls, leading to the pores of modified stomata, is available. A symplastic pathway, via plasmodesmata connecting sieve elements to companion, parenchyma and epidermal cells, is also feasible. Uncollected nectar was reabsorbed, and the direct innervation of the nectary by sieve tubes potentially serves a second important route for nectar-sugar reclamation. Microchannels in the outer cuticle may facilitate both secretion and reabsorption.

Key words: *Echinacea purpurea*, eccrine process, floral nectary, floret phenology, modified stomata, nectar reabsorption, nectar secretion, phloem, ultrastructure.

INTRODUCTION

The purple coneflower, *Echinacea purpurea* (Asteraceae: Heliantheae), is economically important for its medicinal qualities (Kindscher, 1989; Wagner, 1999). Bioactive compounds of interest occur in its flowers, green organs and roots (Bauer, 1998). Seed is essential for this commercial industry, yet the inflorescence's disc florets are almost exclusively self-infertile and must be cross-pollinated by insects (McGregor, 1968). Therefore, to fully understand the attractiveness of the capitulum to insect visitors, nectary structure and nectar secretion in the disc florets must, among other aspects, be identified.

In the Asteraceae (Compositae), floral nectaries are annular, multicellular outgrowths that form on top of the inferior ovary and surround the style base (Frei, 1955; Mani and Saravanan, 1999). Nectary morphology is highly variable, ranging from flat, to cup-shaped, to even, multilobed rings. This variability is depicted in line drawings from 48 species of the family by Gopinathan and Varatharajan (1982) and Mani and Saravanan (1999). Within a capitulum, however, some florets may lack nectary tissue. Also, disc florets tend to produce more nectar than ray florets, which may either lack or possess only a very small nectary (Mani and Saravanan, 1999). A notable exception occurs in *Heterothalamus alienus*, whose ray florets produce an abundance of nectar (Vogel, 1998).

Similarly, the type of vascularization to the nectary is highly variable in Asteraceae (Fahn, 1979); the vascular bundles originate from the style and ovary (Gulyás and Pesti, 1966). Of the 33 species investigated to date, 21 % have their floral nectaries innervated by both phloem and xylem, 27 % by phloem alone, and 52 % lack vascular tissue altogether (Frei, 1955; Kartashova, 1965; Gulyás and Pesti, 1966; Galetto, 1995; Sancho and Otegui, 2000; Ma *et al.*, 2002). Various types of vascularization even exist among species within the same genus (e.g. *Centaurea*; Frei 1955; Gulyás and Pesti, 1966). Despite this internal variation, the nectary surface is very similar; in over 70 asteracean species surveyed (see Davis, 1992), modified stomata may serve as sites for nectar escape from the nectary (Caspary, 1848; Bonnier, 1879; Gopinathan and Varatharajan, 1982; Vogel, 1998; Mani and Saravanan, 1999; Warakomska and Kolasa, 2003).

* For correspondence. E-mail davisa@duke.usask.ca

In spite of the impressive species diversity in the Asteraceae, and their reproductive success promoted by their wide appeal to many generalist pollinators (Proctor *et al*., 1996), plus the family's importance in terms of honey production on a global scale (Crane, 1975; Shuel, 1992), there are only two previous studies (Tacina, 1979; Sammataro *et al.*, 1985) to our knowledge in which floral-nectary ultrastructure was investigated. Both involved the same species (*Helianthus annuus*). Thus, this study represents the second asteracean species for which nectary ultrastructure has been reported. Data on floral nectar production and dynamics in *Echinacea purpurea* are also lacking. Accordingly, the goals of this study were to examine the anatomy and ultrastructure of the floral nectary in relation to nectar secretion, from its commencement to cessation, at three stages of the disc florets of *E. purpurea*, throughout floret phenology.

MATERIALS AND METHODS

Plant material and growth conditions

Plants of *Echinacea purpurea* L. (Moench) utilized for studies of nectar production were transplanted as seedlings (obtained from Helga's Herbs, Saskatoon, SK, Canada) into a plot near the W.P. Thompson building at the University of Saskatchewan in May 2004. Five plants, which initiated flowering by mid-September, were transplanted into individual pots containing Sunshine Sphagnum Mix (Sun Gro Horticulture, Seba Beach, AB, Canada) and placed in a growth chamber at 22 °C day and 16 °C night temperatures with 4305 lx illumination on a 16 : 8 h light : dark cycle. Plants were watered daily and fertilized with 20 : 20 : 20 (N : P : K) fertilizer (Plant-prod, Plant Products Co. Ltd, Brampton, ON, Canada).

For the floral tissues utilized in scanning electron microscopy (SEM) and transmission electron microscopy (TEM) analyses, plants were propagated from seed (Horizon Herbs, Williams, OR, USA) in a greenhouse where they were watered and fertilized as required. Plants were grown under natural light conditions with supplemental lighting provided by fluorescent bulbs.

Determination of disc floret phenology within a capitulum

Seven phenological stages: mature bud, staminate phase (SPi, SPd) and pistillate phase (PP1, PP2, PP3 and PP4) were identified according to the development and relative location of disc florets within an inflorescence (capitulum). Details of the seven stages are provided at the beginning of the Results.

Nectar collection and analysis

To estimate the quantity of nectar sugar per stage of floret phenology encountered by potential pollinators on the capitulum, sampling of nectar was attempted from disc florets of 17 inflorescences from five plants, during three intervals (morning: 0900–1100 h; midday: 1101–1400 h; afternoon: 1401–1900 h) for each phenological stage (Spi + SPd, PP1–PP4). A 0·2 µL microcapillary tube (Drummond Microcaps®) of common bore was inserted into the corolla to its base, and the volume of withdrawn nectar calculated from the height of the nectar column. The nectar was then released onto the prismatic surface of a hand-held refractometer (0–50 % and 40–85 %; Bellingham and Stanley, Tunbridge Wells, Kent, UK), which had been modified by the manufacturer for the measurement of small quantities of nectar. Approximately 90 % of nectar samples yielded a reading on the refractometer. The nectar-solute concentrations obtained were based on weight (NCW) and corrected to 20 °C (manufacturer's reference manual) before conversion to µg sugar per µL nectar (NCV) using the quadratic equation of Búrquez and Corbet (1991). The nectar-sugar quantity per disc floret was estimated as the product of the nectar volume and NCV.

To determine the nectar carbohydrate composition, nectar from three plants was collected separately for each of three phenological stages (SPi + SPd, PP1, PP2) by pooling nectar from several florets per whorl into a 1-µL microcapillary before expulsion onto a filter-paper wick (McKenna and Thomson, 1988). Sampling from these three stages of florets was achievable from consecutive whorls within the same inflorescence, thereby allowing comparison of nectar-carbohydrate composition within a genotype. Stored wicks were later eluted individually in 2-µL Eppendorf tubes containing 150–1000 µL of pure distilled water, depending on the dilution required to allow carbohydrate peaks to fall within the range of standard curves created for each major nectar sugar (glucose, fructose, sucrose; 5–200 ppm). After filtering, 50 µL of each sample was analysed in duplicate using a Waters HPLC system, as described in Davis *et al*. (1998).

Nectary structure: SEM

For detailed studies of nectary morphology, nectaries from disc florets in three distinct phenological stages (mature bud, SPd and PP1) were removed from mature capitula of two plants and processed for SEM. Floral organs were removed to expose the nectary prior to fixation. Dissected florets were fixed in 2 % glutaraldehyde (GA) in 25 mM Na phosphate buffer, pH 6·8, for a minimum of 0·5 h. After rinsing three times with buffer, tissues were post-fixed for 2 h in 1 % OsO_4 in buffer. Three rinses each of buffer and distilled water were followed by dehydration in a graded series of acetone. Tissues were critical-point dried with liquid CO_2 (Polaron Instruments, Watford, UK), mounted on aluminum stubs with two-sided tape, coated with gold (Edwards S150B Sputter Coater), observed with a Philips SEM 505 at 30 kV, and photographed with Polaroid 665 positive/negative film. Negatives and positives were scanned (Epson 3200 Photo) and images edited using Adobe® Photoshop® 7·0. Nectary dimensions and the number and developmental stages of the modified stomata on the nectary surface were compared between floret phenological stages.

Nectary structure: light microscopy and TEM

Disc florets of three distinct phenological stages (SPi – within 1 h following anthesis; late SPd – 24 h after anthesis,

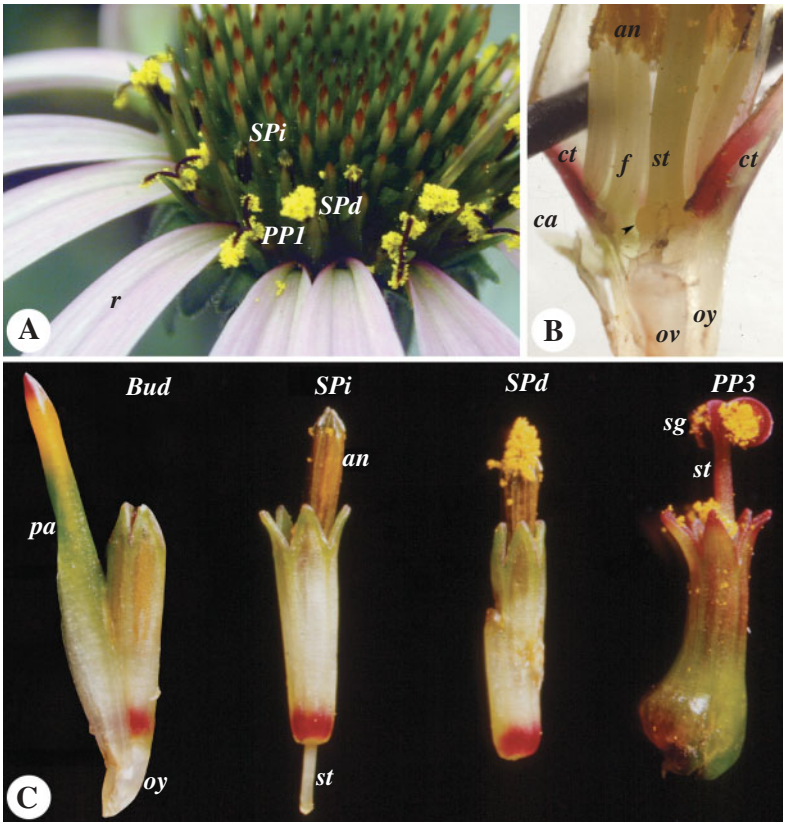

FIG. 1. (A) Inflorescence of *E. purpurea* showing disc florets of the indehiscent staminate phase (SPi), dehiscent staminate phase (SPd), first day of the pistillate phase (PP1) and ray florets (r). (B) Disc floret dissected to show the tubular corolla (ct), adnate filaments (f) and anthers (an) containing pollen, style (st), ovary (oy), single ovule (ov) and nectary (arrow). (C) Disc florets from four phenological stages: mature bud with palea (pa), indehiscent staminate phase (SPi) with style base (st) visible, dehiscent staminate phase (SPd) and third day of the pistillate phase (PP3) with recurved stigmas (sg). Ovary (oy) present on bud and removed elsewhere.

as pollen accumulated on the pre-receptive stigma lobes; early PP2 – 48 h post-anthesis, with stigma lobes fully bifurcated and receptive) were harvested from the same inflorescence and dissected to expose the nectary on top of a cross-sectioned ovary. Tissues were fixed in 1·5 % GA in 25 mM Na phosphate buffer, pH 6·8, for 0·5 h at room temperature, before transferring to 3 % GA in buffer for 2 h. On ice, samples were rinsed with buffer over 1–12 h, post-fixed overnight with 1 % OsO_4, then rinsed with distilled water before dehydration in an ethanol series. A gradual substitution of ethanol by propylene oxide preceded sample infiltration and embedding in Araldite 502 resin at 60 °C for 24 h.

For light microscopy, semi-thin (0·5–1 µm) sections of floral nectaries, cut with glass knives on a Reichert OMU3 ultramicrotome, were heat-fixed to microscope slides, stained with toluidine blue, and then mounted in immersion oil under coverslips. Sections were examined with a Zeiss Universal microscope and photographed with Fujifilm Superia ISO 100 film.

For TEM, ultrathin (70–90 nm) sections were floated onto copper grids and air-dried before staining in 2 % uranyl acetate and lead citrate (Reynolds, 1963). Sections were examined using a Philips TEM 4101 LS and photographed with Kodak film. Micrographs were processed electronically as for SEM (above).

RESULTS

Phenology and morphology of ray and disc florets

The cone-shaped capitulum of *E. purpurea* began anthesis with the maturation of the outer, single whorl of sterile, ligulate (ray) florets, which surround multiple whorls of fertile, bisexual disc florets (Fig. 1A). Mean number of disc florets per capitulum was 276 ± 19 (n = 10). Each disc floret is subtended by a bract (palea) (Fig. 1C, left), which gives the capitulum's centre an echinate appearance (Fig. 1A). Disc florets mature sequentially, in whorls, from the periphery of the capitulum to the centre, with one whorl of florets reaching anthesis (corolla opening) in the morning of each day. Development of the disc florets is protandrous; mature buds pass through a staminate phase on the first day of anthesis followed by a pistillate phase, which begins on the second day (Fig. 1A and C). The staminate phase is characterized by stamen elongation which causes extension of the tube of indehiscent anthers (SPi) beyond the corolla lobes of the mature bud, followed swiftly by anther dehiscence and pollen presentation (SPd) (Fig. 1C). On the following day, the style elongates, forcing the unreceptive (closed) stigma lobes through the anther tube and pollen mass before the stigma lobes reflex and become receptive (Fig. 1A), which occurs on the first day of the pistillate phase (PP1). Disc florets remained in the pistillate phase

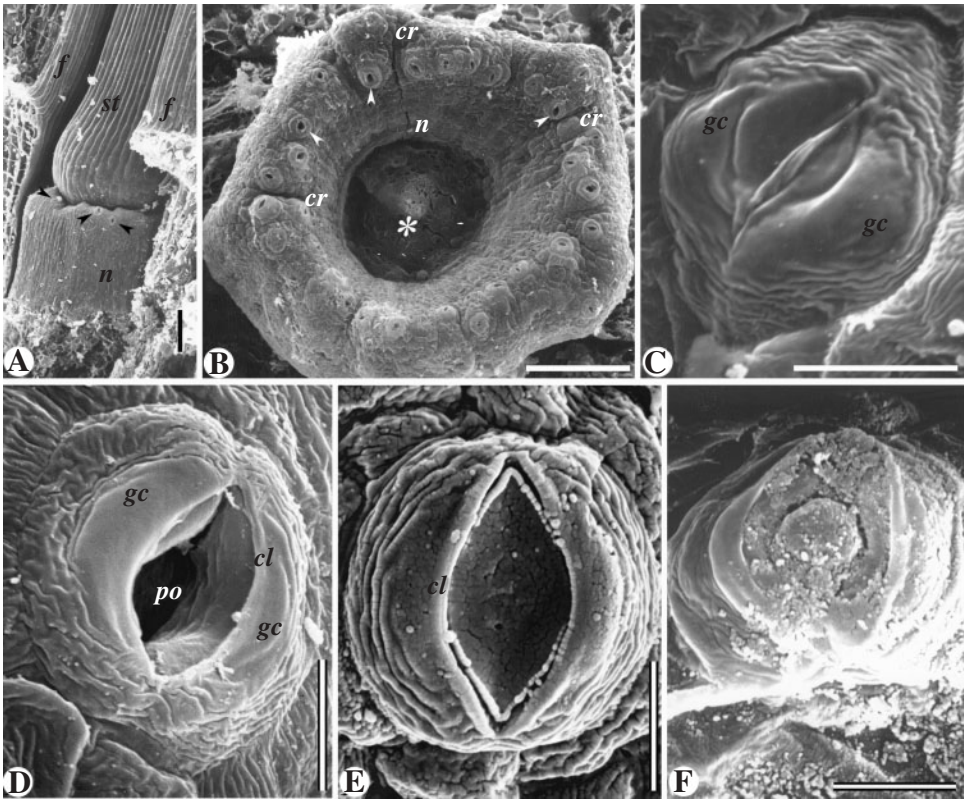

FIG. 2. SEM micrographs of the floral nectary of disc florets of *E. purpurea*. (A) Dissected disc floret showing the floral nectary (n) from the side, below the swollen base of the style (st). Modified stomata (arrows) along the nectary rim. f, Filaments. (B) Floral nectary (n) from above (style removed); bud phase. Modified stomata (arrowheads) especially located along the rim; note depression (asterisk) where the style base resided. Cr, Nectary creases. Scale bars = 0·1 mm. (C–F) Developmental stages of modified stomata. (C) Immature stomate with intact cuticle between guard cells (gc). (D) Mature stomate with open stomatal pore (po) and guard cells (gc) with cuticular ledge (cl). (E and F) Mature stomata demonstrating pore occlusion. Scale bars = 10 µm.

for several days until senescence or cross-pollination occurred, whereby the stigmas and style shrivelled and withdrew into the corolla tube as it senesced. Stages PP2, PP3 (Fig. 1C) and PP4 marked the second, third and fourth days of stigmatic receptivity, and the third, fourth and fifth days of flowering, respectively.

The filament bases of the five fused anthers were adnate to the bases of the five petals (Figs 1B and 2A, left) of each disc floret. The petals were fused into a campanulate corolla (Fig. 1C) whose base gradually enlarged (Fig. 1C, right) and functioned as a nectar reservoir. Although absent in the ray florets, a yellowish nectary formed around the style base of the disc floret (Fig. 2A) on top of the inferior ovary (Fig. 1B). From above, the floral nectary had a pentagonal, cup-shaped appearance (Fig. 2B) with a collar-like profile (Fig. 2A). It was about 360 µm at its widest point and 122–154 µm high (Table 1). The five-sided nature of the nectary was attributed to its formation following establishment of the pentamerous corolla base that surrounded it. The inner surface of the nectary, however, had a more regular, circular circumference as it molded around the cylindrical style (Fig. 1B). The shape of the style, whose inserted, tapered apex of the base (Fig. 1C, bottom of SPi stage) below a dilated portion of the style base slightly higher up (Fig. 2A) may also reflect growth pressure on this organ, exerted by the expanding nectary.

Dynamics of nectar secretion

Plants of *E. purpurea* grown in a growth chamber under a regular light and temperature regime were not subjected to environmental fluctuations that are typical of field conditions. Thus, the major variable contributing to nectar production of disc florets in this study was the result of floral phenological stages, rather than environment. Figure 3A illustrates mean nectar volume per disc floret spanning the commencement of nectar accumulation (morning of the staminate phase SP) to the cessation of nectar production by the end of the third day of the pistillate phase (PP3), 4 d post-anthesis.

At anthesis, disc florets in the staminate phase (SPi and SPd) held an average of 0·07 µL of nectar that increased to 0·15 µL later that first day (Fig. 3A). Nectar volume declined overnight, reaching 0·1 µL in the morning before rising significantly to 0·19 µL (midday) and 0·18 µL (afternoon)—the peak values for disc florets—on the second day post-anthesis (PP1). On the second day of the pistillate phase (PP2), nectar volume remained significantly lower and fairly constant at about 0·1 µL per disc floret, before declining to 0·05 µL during the third day of the pistillate stage (Fig. 3A), when only 24 % of sampled florets yielded nectar. All florets lacked nectar by the fourth day of stigma receptivity (PP4) (Fig. 3A). Regardless of the stage

TABLE 1. *Dimensions (mean ± s.e.) of the floral nectary of* E. purpurea *and developmental stages and dimensions of its modified stomata at three phenological phases of disc florets*

			Modified stomata						
	Nectary dimensions (μm)		Number per developmental stage (%)				Dimensions (μm)		
Phenological stage of floret	Exterior width	Height	Total	Immature	Open	Occluded	Width	Length	Pore width
Mature bud	357·5 ± 17·5	137·0 ± 35·0	32·5 ± 4·2	2·8 ± 2·1 (8·3)	28·5 ± 4·7 (87·7)	1·3 ± 0·5 (4·0)	19·8 ± 0·6	21·1 ± 0·7	2·79 ± 0·30
Staminate	367·5 ± 14·4	154·0 ± 22·5	26·8 ± 0·5	2·5 ± 0·9 (9·3)	21·8 ± 0·8 (81·3)	2·5 ± 0·3 (9·3)	19·8 ± 0·5	21·6 ± 0·4	1·71 ± 0·11
Pistillate	362·3 ± 24·5	121·5 ± 12·1	28·3 ± 1·7	2·0 ± 1·2 (7·1)	21·8 ± 2·5 (77·0)	4·5 ± 1·4 (15·9)	22·3 ± 0·5	22·2 ± 0·8	2·43 ± 0·29

Four florets are represented per phase.
Stomatal measurements were taken from seven open stomata per nectary.

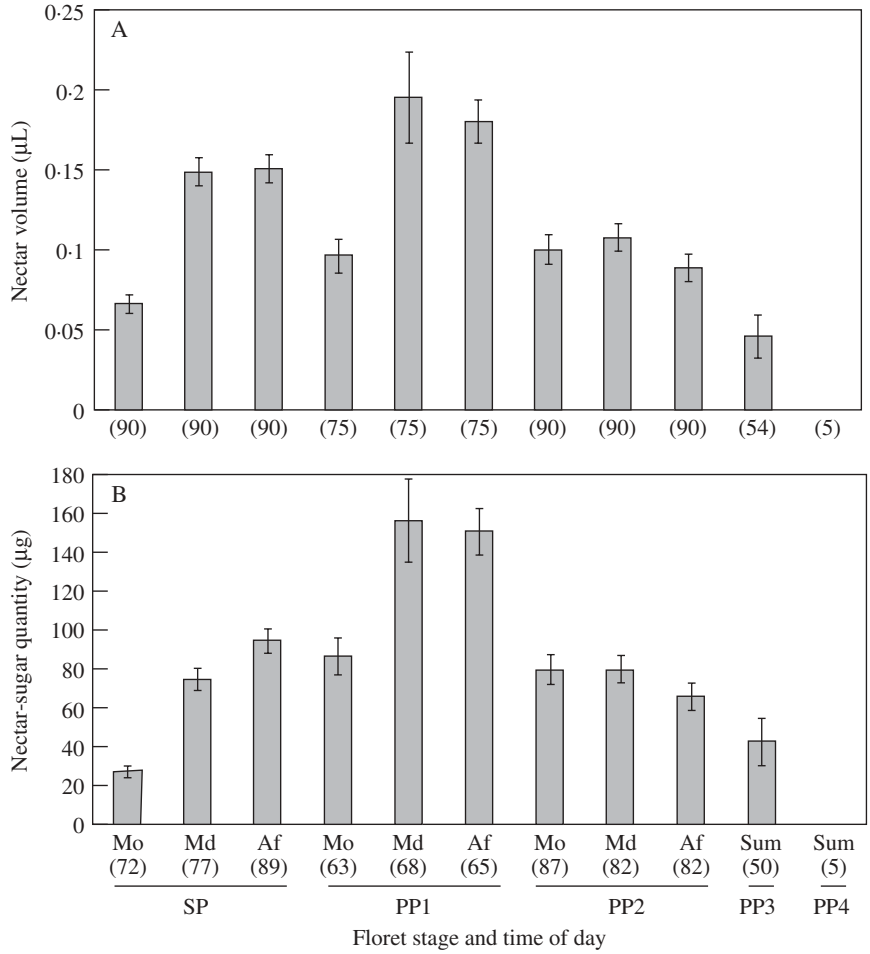

FIG. 3. Nectar characteristics of disc florets of *E. purpurea*. (A) Nectar volume (mean ± s.e.). (B) Nectar-sugar quantity (mean ± s.e.). Mo, Morning; Md, midday; Af. afternoon; SP, staminate phase; PP1first day of the pistillate phase; PP2, second pistillate phase; PP3, third pistillate phase; PP4, fourth day of the pistillate phase. The numbers in brackets represent the total number of disc florets sampled (A) and all sampled florets except those that failed to yield sufficient nectar for refractometry (B) per floret stage and time of day. Many of the SP (Mo) florets were indehiscent; all other staminate phase florets were dehiscent.

of floret development, on a daily basis, nectar volumes tended to be highest at midday (Fig. 3A).

Average nectar-solute concentrations (refractometer measurements) rose throughout the staminate phase (SP) of disc florets from 33·4 % (morning) to 43·2 % (midday) and 53 % (afternoon). However, from the first day of the pistillate phase (PP1) to the end of nectar secretion, nectar-solute concentrations remained constant ($P = 0{\cdot}204$, $\alpha = 0{\cdot}05$), averaging 61·1 ± 1·1 %.

Nectar-sugar quantity per disc floret rose from 26·9 μg in the first h after anthesis to 94·3 μg by the afternoon of the staminate phase (SPd) (Fig. 3B). Owing to the consistency

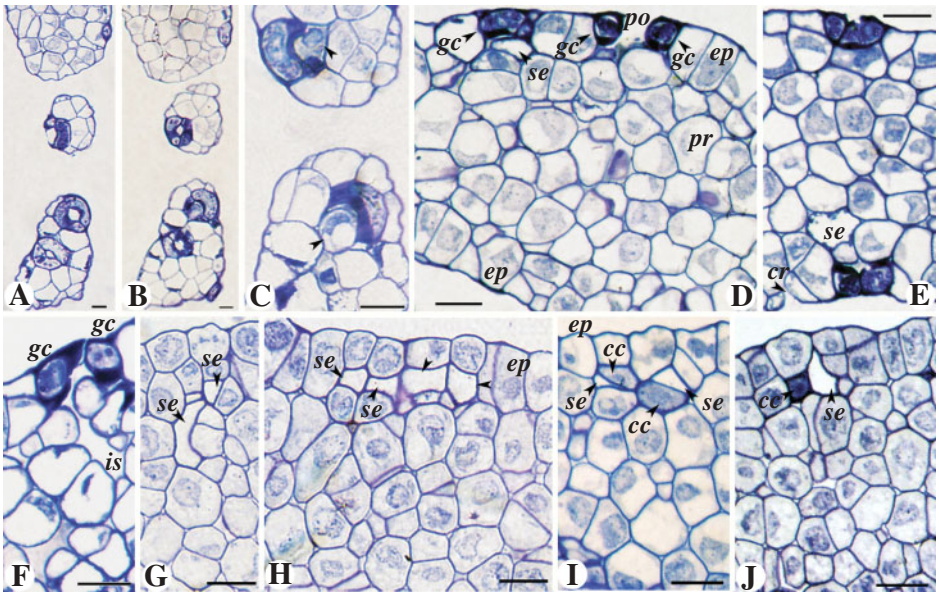

FIG. 4. Light micrographs of transverse sections through the floral nectary of a pistillate phase (PP2) floret of *E. purpurea* stained with toluidine blue. (A–C) Serial sections through the rim of the floral nectary showing stomata and parenchyma of the nectary rim: (C) parenchyma cells (arrowheads) evident directly beneath the stomatal apertures. (D–F) Immediately below the apical rim where stomata are sectioned in various planes: (D) two stomata on the outer epidermis of the nectary and outer (uppermost) and inner (lowermost) epidermal layers (ep) with intervening parenchyma cells (pr); guard cells (gc) and stomatal pore (po) – possible sieve element (se) below guard cells at top left; (E) stomata on the outer and inner nectary surfaces and sieve element (se) near stomate on inner epidermis – note the crease (cr) in the inner epidermis; (F) substomatal chamber is continuous with a large intercellular space (is). (G–J) Mid-region of the floral nectary: (G) sieve tube of elements (se) branching toward the epidermis; (H) four sieve tube elements (se) next to the outer epidermis (ep); (I) two sieve elements (se) of a sieve tube and their darkly staining companion cells (cc) adjacent to the outer epidermis; (J) a companion cell and adjacent sieve element intervening the bases of cells of the nectary's outer epidermis. Scale bars = 10 μm.

in nectar-solute concentration throughout stigma receptivity, thereafter nectar-sugar quantity per disc floret (Fig. 3B) closely mirrored the pattern of nectar volume (Fig. 3A). Thus, peak quantities of nectar sugar per floret occurred at midday (156·6 μg) and afternoon (150·7 μg) of PP1 (Fig. 3B). The following day, after midday, 80 μg of nectar sugar per floret fell to 65·9 μg in the afternoon of PP2, and decreased to 42·5 μg on the third day of stigma receptivity (PP3) before cessation of nectar production by the fourth day (PP4) (Fig. 3B).

Nectar-carbohydrate composition

The floral nectar of all disc-floret stages (SPi + SPd, PP1, PP2) contained glucose (G), fructose (F) and sucrose (S). Nectar was dominated by the hexose sugars throughout flowering phenology, with a reduction in sucrose content as florets aged. For example, from one capitulum, the G : F : S ratio of floral nectar sampled separately from distinct phenological stages located in three adjacent whorls was 1·8 : 2·0 : 1, 3·3 : 3·4 : 1 and 3·9 : 4·1 : 1, respectively.

Nectary anatomy and ultrastructure

The multicellular floral nectary of *E. purpurea* consists of three distinct tissues: (1) the epidermis; (2) a direct supply of phloem; and (3) a large region of secretory parenchyma located within the interior.

Epidermis

This single cell layer was composed of modified stomata dispersed among non-specialized epidermal cells. Trichomes, and subsidiary cells around the paired guard cells per stomate, were absent.

On average, 29·2 modified stomata were present on the nectary surface, and the data in Table 1 suggest that additional modified stomata are not initiated after the mature bud phase is attained. The modified stomata were densest along the uneven upper rim of the nectary (Figs 2A and B and 4A and B), although they were oriented in different planes and were rarely adjacent to one another (Figs 2B and 4A and D). Less frequently, stomata were located below the nectary rim, positioned on both the exterior and interior nectary surfaces (Figs 2B, bottom right, and 4E). Along the rim, the two kidney-shaped guard cells of each modified stomate were slightly raised (Fig. 2B and D–F), but were not raised in those stomata located on the external and internal walls of the nectary (Figs 4D and E). Each guard cell possessed a centrally located nucleus (Fig. 4C, top left, and D, top right) and abundant amyloplasts (Fig. 4A–F).

The surface of the guard cell varies: closest to the pore it is smooth while it is covered with circumferential ridges in the region closet to the non-specialized epidermal cells (Figs 2C–E). Sometimes the overlying cuticle between the two guard cells of an immature modified stomate was folded (Fig. 3C), rather than taut, possibly an indication of a reduced guard-cell turgor during fixation and dehydration. As guard cells expanded, this outer cuticle was stretched and eventually could be torn to reveal the pre-formed pore below (Fig. 2D). Each guard cell possessed an outer ledge on its relatively thick ventral wall lining the pore

(Fig. 4D, top right), which demarcated the future (Fig. 2C) and actual (Fig. 2D and E) site of cuticle rupture.

Various stages of stomatal development were encountered on nectaries examined from mature bud to pistillate-phase florets (Table 1): immature stomata in which the pore was still covered by the cuticle (Fig. 2C); stomata with visibly open pores (Figs 2D and 4A, B and D, top right); and stomata with the pore occluded and not visible (Fig. 2E and F). On average, 7·1–9·3 % of stomata remained immature even in actively secreting glands (Table 1). The majority (87·7 %) of the nectary's modified stomata are already open, even in the mature bud phase (Table 1) before nectar secretion began. Nectar presumably exudes through some or all of the unblocked stomatal pores.

Stomatal pores do not appear to close by guard-cell movements, and pores can still remain open after nectar secretion has ceased. However, pores may become occluded (up to 16 % of stomata in the pistillate phase) (Table 1), in different ways that evidently block nectar flow. Figure 2E demonstrates the occlusion of a stomatal pore with unknown material completely filling the area below the bases of the cuticular ledges. Occlusion may also occur from below, by a plug of material that protrudes beyond the ledges (Fig. 2F); it is possible that a portion of a parenchyma cell normally underlying the guard cells (Fig. 4C, D and F) may contribute to stomatal pore occlusion in such instances.

Serial sections (Figs 4A–C) demonstrated that the substomatal space below a modified stomate was typically small, owing to contact maintained between the guard cells and parenchyma cells immediately below (Figs 4D and E). Below an obliquely sectioned stomate, however, a continuous passage connecting the diminutive substomatal space with a larger intercellular space among the nectary's parenchyma cells was evident (Fig. 4F).

The majority of the epidermis comprised less differentiated, compact, tight-fitting cells (Fig. 4D and G–J). Recesses representing a limited number of creases particularly along the nectary's interior wall and rim (Fig. 2B) permit contact of subepidermal cells to the exterior, between slightly separated epidermal cells (Fig. 4E, bottom left).

The surface of the epidermal cells was ornamented by ridges (Fig. 2C–E), usually oriented along the cell's length, and similar in pattern to the circumferential ridges on the outer walls of adjacent guard cells (Fig. 2C–E). Part of a ridge is evident in Fig. 5B (top right) and consists of a thickening of the external primary wall, covered throughout by an osmiophilic cuticle (Fig. 5A–C) of 185 ± 10 nm thickness. Above a junction of anticlinal walls of non-guard epidermal cells, the deposition of osmiophilic globules (possibly pre-cuticle components) beneath an established layer of cuticle was evident (Fig. 5D). The cuticle had a bipartite nature, consisting of a very fine, intact epicuticular layer (42·6 ± 4·0 nm) subtended by a thicker (142 ± 11 μm) layer regularly interrupted by channels reaching the epicuticle (Fig. 5D). These thicker regions of wall above the anticlinal wall junctions stained lightly (Fig. 5C and D) or densely osmiophilic (Fig. 5A).

Each epidermal cell typically possessed a single, large vacuole (Figs 4C–E) traversed by cytoplasmic strands (Fig. 5A, left). Occasionally, various vacuolar inclusions such as multitubular and multilamellar bodies, as well as a flocculant material, occurred (Fig. 5A). In the cytoplasm, a prominent nucleus of spherical (Fig. 4G and H) or more irregular (Fig. 4D and E) shape, resided. An abundance of ribosomes in the ground substance gave the cytoplasm a dense and granular appearance (Fig. 5A–D). Mitochondria with prominent cristae (Fig. 5A–D) and plastids with plastoglobuli but very few thylakoid membranes (Fig. 5B) were abundant organelles. Microbodies (Fig. 5B), rough endoplasmic reticulum (Figs 5A, B) and dictyosomes (Fig. 5B and C) were also evident. The latter were common in the vicinity of the cell membrane (Figs 5B and C). The irregular internal surface of the cell membrane and primary wall beneath (Fig. 5A–D) may reflect cell-wall deposition involving dictyosome vesicles. Plasmodesmata traversed the walls between epidermal cells (not shown) and between epidermal cells and the nectariferous parenchyma cells below (Fig. 5A).

Nectary vasculature

Certain developmental features of the nectary phloem are noteworthy. Depending on the particular phloem trace, contact between a sieve tube and the epidermis occurs primarily via the sieve tube elements (Fig. 4H and I, right), or less commonly by the companion cells (Figs 4G and I, left, and 5A), or sometimes by both almost equally (Fig. 4J). Sometimes the sieve tubes are oriented horizontally (Fig. 4H) and have been seen to yield vertically oriented traces leading higher up within the nectary at each of their ends (data not shown). In these horizontally oriented sieve tubes, the origin of the sieve element–companion cell precursor cells can be inferred from epidermal cells on the outer nectary surface (Fig. 4H). Based on their common widths between anticlinal walls, the epidermal cells above these four sieve elements had divided periclinally, evidently to yield the sieve element–companion cell precursors which themselves subsequently have divided periclinal to the outer surface, to form companion cells below the sieve elements. That multiple companion cells may eventually arise per sieve element is suggested from the two rightmost sieve elements, which are superior to at least two smaller companion cells each (Fig. 4H). Meanwhile, epidermal cells to the left and right of the mature sieve elements remain columnar (Fig. 4H), possibly delineating the original size of the four epidermal cells between them, which have participated in the formation of phloem.

Mature sieve elements of the nectary interior were anucleate (Fig. 6A) and possessed a peripheral cytoplasm (Figs 4E and 6A) that included organelles such as plastids (Figs 5A and 6A, top), mitochondria (Fig. 6A, centre, and D) and endoplasmic reticulum (Fig. 6D and E). The lumen contained p-protein (Figs 5A and 6A, B and D). The sieve plate between sieve elements contained pores lined by unstained (white) callose (Fig. 6A). Sieve elements were connected by plasmodesmata to phloem parenchyma (Fig. 6A, bottom left) and companion cells (Figs 6D, E). Intercellular spaces occurred next to sieve elements (Figs 4E, 6A, top, and B).

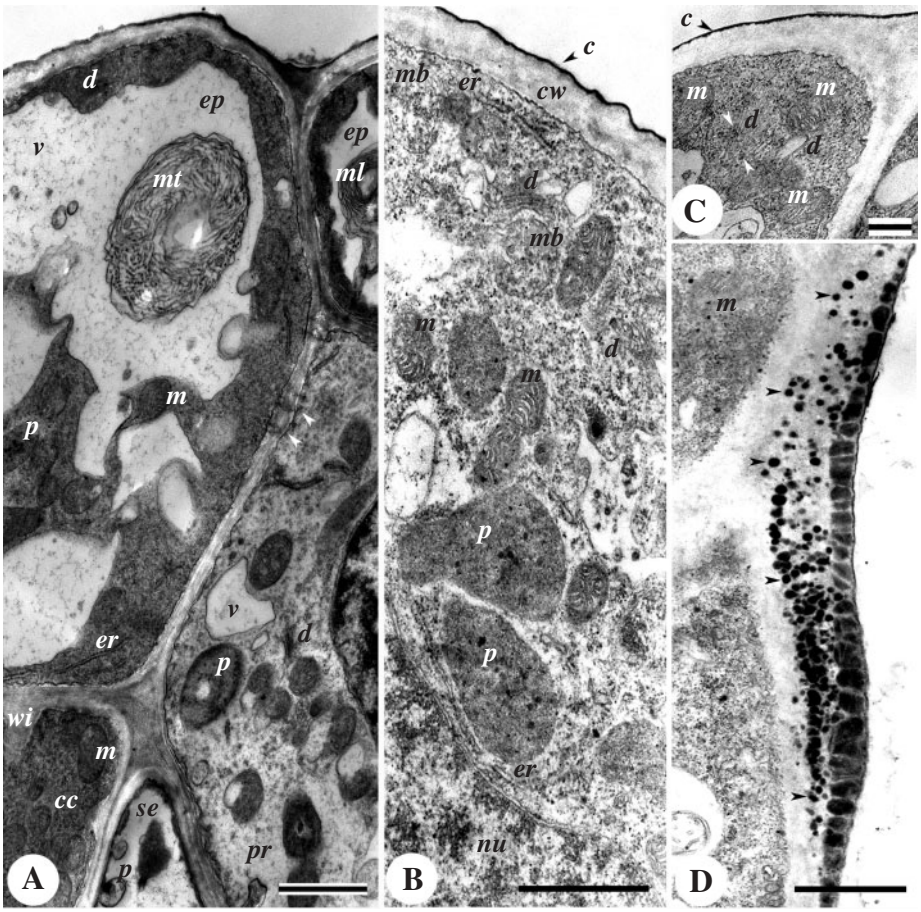

FIG. 5. Transmission electron micrographs (TEM) of the epidermis of floral nectaries of *E. purpurea.* (A) Epidermal cells (ep) showing mitochondria (m), plastids (p) and rough endoplasmic reticulum (er) in association with ribosomes, and membranous multilamellar (ml) and multitubular (mt) bodies within large vacuoles (v). Plasmodesmata (arrows) evident in the wall between epidermal and phloem parenchyma cell (pr). Sieve element (se) with plastids (p) and companion cell (cc) with mitochondria (m) and wall ingrowth (wi) next to epidermis. PP1 phase. Scale bar = 1 µm. (B) Epidermal cell with thin cuticle (c) covering the outer wall (cw), plastids (p) containing electron-dense plastoglobuli, rough endoplasmic reticulum (er), dictyosomes (d), mitochondria (m), microbodies (mb) and nucleus (nu). SPi phase. Scale bar = 1 µm. (C) Note thin cuticle (c), and mitochondria (m), dictyosomes (d) surrounded by vesicles (arrowheads) and unevenness of the anticlinal wall between the two epidermal cells. SPd phase. (D) Outer junction of two epidermal cells showing deposition of osmiophilic globules (arrowheads) along the outer walls. Microchannels evident in cuticle. SPi phase. Scale bars = 0·2 µm.

Companion cells were either larger than (Fig. 4I), similar in size (Fig. 6A) or dwarfed by (Fig. 4H, right) their adjacent sieve elements. The dense-staining cytoplasm contained plentiful ribosomes in its ground substance (Fig. 6C and E), as well as a prominent nucleus (Figs 4H and I and 6A, top, and C), mitochondria (Figs 5A and 6A and C) and dictyosomes (Fig. 6E). Their small vacuome (Fig. 6A and E) contained a flocculent material, and inclusions ranging from multiple vesicles (Fig. 6E, left) to multilamellar bodies (Fig. 6E, right).

Characteristics of the companion-cell walls were also noteworthy. Companion cells were the only nectary cells to be modified as transfer cells (Type A; Gunning and Pate, 1969), their wall ingrowths consisting of secondary wall material on top of the primary wall (Figs 5A and 6E). The wall ingrowths were directed toward epidermal cells (Fig. 5A), phloem parenchyma (Fig. 6A and E), and other companion cells (Fig. 6A, top), but never toward sieve elements (Figs 5A and 6A and E). Putative plasmalemmasomes (Fig. 6C) and vesicles below the cell membrane (Fig. 6C, top right) also occurred at the primary wall. Plasmodesmata connected companion cells to sieve elements (Fig. 6D and E) and phloem parenchyma (Fig. 6C). Intercellular spaces were also located next to companion cells (Fig. 6A and C).

Parenchyma cells adjacent to sieve elements and companion cells were typically larger and less densely stained (Figs 5A and 6A), and were designated as phloem parenchyma. These cells had very similar features to the parenchyma cells (see below) that formed the remainder of the nectary. Phloem parenchyma cells often contained a multilobed nucleus (Fig. 7B), fibrillar proteinaceous material (Fig. 6B), dictyosomes (Figs 5A, 6E and 7B), mitochondria (Figs 5A, 6B and E, bottom right, and 7B), endoplasmic reticulum (Fig. 6B and C) and plastids (Figs 5A and 6A) that can contain starch (Fig. 7B). Phloem parenchyma cells were connected by plasmodesmata to sieve elements (Fig. 6A and B), companion cells (Fig. 6C) and epidermal cells (Fig. 5A), and they also opposed intercellular spaces (Fig. 6A–C).

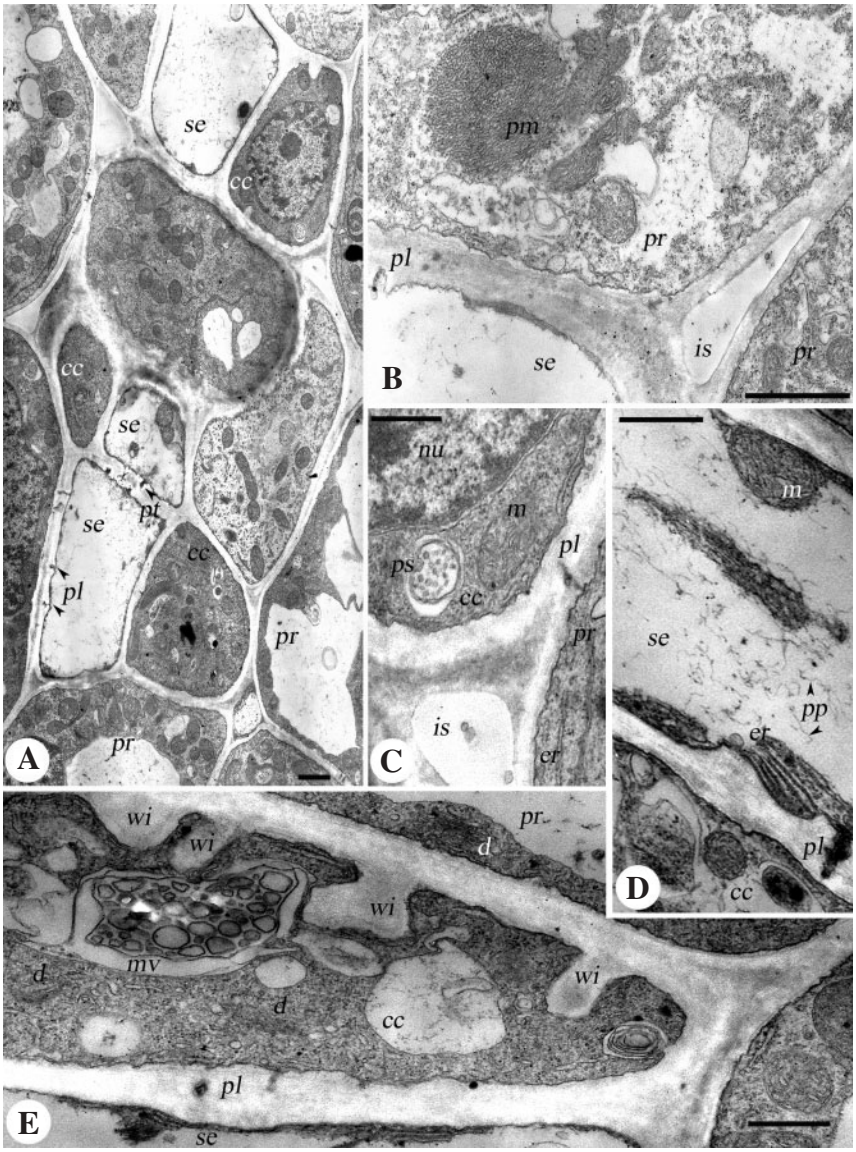

FIG. 6. TEM highlighting the vascular tissue of floral nectaries of *E. purpurea*. (A) Nectary interior showing portion of a sieve tube with pores of a sieve plate (pt) between adjacent sieve elements (se). Companion (cc) and parenchyma (pr) cells. PP1 phase. (B) Sieve element (se) next to an intercellular space (is) with parenchyma cells (pr), part of a plasmodesma (pl) and proteinaceous material (pm) at the SPi phase. Scale bars = 1 μm. (C) Companion cell (cc) with nucleus (nu), mitochondrion (m) and possible portion of a plasmalemmasome (ps), and plasmodesma (pl) connecting companion cell with parenchyma cell (pr) at the PP1 phase. er, Rough endoplasmic reticulum. Scale bar = 0·5 μm. (D) Peripheral cytoplasm of a sieve element (se) containing endoplasmic reticulum (er) and a mitochondrion (m) adjacent to a companion cell (cc) at the PP1 phase. pp, P-protein in the lumen; pl, plasmodesma. Scale bar = 1 μm. (E) Companion cell (cc) with wall ingrowths (wi) opposing a parenchyma cell (pr), dictyosomes (d), a multivesicular inclusion (mv) in vacuole, portions of plasmodesmata (pl) between sieve element (se) and companion cell, and peripheral cytoplasm visible in sieve element at the PP1 phase. Scale bar = 0·5 μm.

Parenchyma cells

Thin-walled parenchyma cells comprised the bulk of the nectary interior (Figs 4D–J). Each cell contained a dense-staining nucleus, often spherical (Figs 4I and 7A) or lobed (Figs 4H and J and 7B), with multiple dense nucleoli (Fig. 4E, H and J). Plastids were homogeneous with osmiophilic plastoglobuli (Figs 7A and 8A–C), very few thylakoids (Fig. 8A–C) and lacked starch (Fig. 7A) or possessed a single starch grain per plastid profile (Figs 7B and 8B). Plastids commonly were lobed (Fig. 8A) and often surrounded a mitochondrion (Figs 6A, top right, and 8C, top right). Mitochondria were very abundant and had well-developed cristae (Figs 7A and 8A and B). Dictyosomes (Figs 7A and B and 8A and B), rough endoplasmic reticulum (Fig. 7A) and microbodies (Fig. 8A) were also common. Each cell contained a large vacuole (Figs 4D–F and I and 8C) or multiple small vacuoles (Figs 4H and J, 7A and 8A). Many vacuoles contained a flocculent material (Fig. 8A–C). Inclusions of variable form were occasionally present. A multilamellar body was continuous with a multitubular body next to a vacuole (Fig. 8B), indicating that the two inclusions may intergrade. In other examples, cells with the nucleus confined to the periphery and

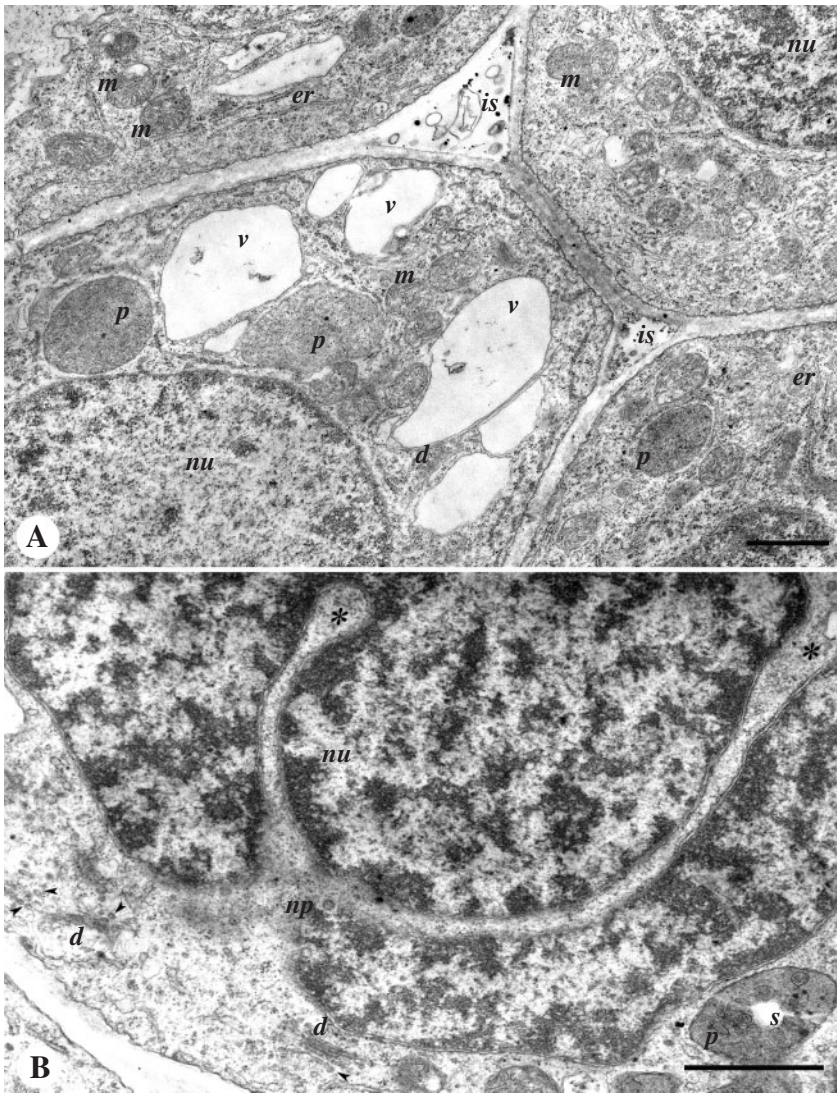

FIG. 7. TEM of the parenchyma of floral nectaries of *E. purpurea.* (A) Nuclei (nu), vacuoles (v), plastids (p), mitochondria (m), dictyosome (d) and rough endoplasmic reticulum (er). Intercellular spaces (is) containing amorphous material. SPi phase. (B) Nucleus (nu) with three prominent lobes encompassing cytoplasm (*). Nuclear pores (np) in nuclear membrane. Dictyosomes (d) and vesicles (arrowheads). Plastid (p) with starch grain (s). PP1 phase. Scale bars = 1 μm.

containing several membrane-bound inclusions (Fig. 8C) may indicate a stage of degradation. Plasmodesmata occurred between parenchyma cells (Figs 7A and 8B and C). Intercellular spaces were located between parenchyma cells (Fig. 4F), sometimes with apparently cellular debris (Fig. 7A) and darkened regions where the middle lamella ended (Fig. 8B and C).

DISCUSSION

Phenology and nectar-production dynamics

The asteracean capitulum is a highly modified aggregation of small florets that creates the illusion of one large flower to attract pollinators. The outer ray florets attract insects visually but typically are sterile, and lack an androecium, gynoecium and nectary. Instead, pollinators are rewarded by pollen and nectar when the inner disc florets are in the staminate phase and, to a lesser extent, in the following pistillate phase (nectar, and collection of any residual pollen available as secondary presentation on the style below the stigmas; Pacini, 1996). Nectar is produced by individual disc florets in small volumes, which entices insects to visit more than one floret, and often more than one inflorescence per foraging trip in order to become satiated. In this way, one insect may transfer pollen grains to many disc florets on other plants of the same species.

In *Echinacea purpurea*, nectar was available continuously from disc florets for up to 4 d, commencing on the morning of anthesis during the indehiscent staminate phase (SPi) and ceasing production after the third day of stigma receptivity (PP3). The actual pattern of nectar production observed can be correlated to the potential pollination of florets by insects in the field. For example, a functional

FIG. 8. TEM of parenchyma cells of floral nectaries from disc florets of *E. purpurea* in the pistillate phase (PP1). (A) Lobed plastids (p) enveloping cytoplasm (*).m, Aggregation of mitochondria; d, dictyosome; mb, microbody. (B) Multitubular (mt) and multilamellar (ml) bodies apparently enclosed by a continuous membrane that abuts the tonoplast of a vacuole (v); also plastids (p) containing starch grains (s), mitochondria (m), dictyosome (d), nucleus (nu) and plasmodesmata (pl) between parenchyma cells. is, Intercellular space. (C) Parenchyma cell with vacuole (v) containing many membrane-bound inclusions possibly undergoing degradation. nu, Nucleus; pl, plasmodesmata. Scale bars = 1 μm.

benefit might be low if the disc florets provided a higher quantity of nectar at SPi, because pollen is not yet presented for distribution. Mani and Saravanan (1999) instructed, however, that in some Asteraceae the probing insect proboscis may stimulate the filaments of indehiscent stamens to contract, typically leading to dehiscence. The rapid rise in nectar volume and concentration throughout the first day, concurrent with anther dehiscence (SPd), could serve to enhance pollen dissemination by insect vectors.

Throughout disc-floret phenology, the quantity of nectar sugar approximated a normal distribution, centred at mid-day/afternoon of the first day of the pistillate stage (PP1). After pollen collection by insects during the staminate phase (SP), nectar becomes the major reward available thereafter. A relatively large nectar quantity in disc florets immediately external to the whorl of SP florets could enhance microgametophyte transfer to other capitula by pollen-laden insects to stigmas on their first day of receptivity (PP1). At PP2, a reduction in nectar-sugar quantity per floret to levels comparable with the late-SP and early-PP1 stages could prolong insect attention to this pistillate-phase whorl in events such as missed pollination or poor foraging conditions. The marked decline in nectar-sugar quantity at PP3 and complete cessation of nectar production by PP4 may result in a loss of potential pollination in a minority of florets, but likely encourages insect interest in the richer,

less-pollinated whorls in the centre of the capitulum, situated more distantly from the visually attractive ray florets. Accordingly, nectar-secretion dynamics in *E. purpurea* appear to represent a classic example whereby events among adjacent whorls of disc florets of the capitulum mimic the succession of reproductive events occurring temporally within an individual flower (Proctor *et al*., 1996).

Various, established physiological and environmental phenomena may account for the pattern of floral nectar secretion in *E. purpurea*. In a growth chamber where pollinators were absent, disc florets produced nectar at a high rate from late morning throughout the afternoon on each of the first two days (SP, PP1) of anthesis, perhaps in relation to plant photosynthesis (Pacini *et al*., 2003). The concurrent increase in nectar-solute concentration throughout SP might be attributable to water evaporation from accumulating nectar. Moreover, the lower nectar volumes on the mornings of PP1 and PP2, compared with the previous afternoons, also may reflect some water loss from nectar, by evaporation. However, during these same intervals, a marked decrease in nectar-sugar quantity by morning, also evident during consecutive days in sunflower (Hadisoesilo and Furgala, 1986), suggests a net reabsorption of nectar sugar. Nectar-sugar reabsorption occurs most frequently in species when contact between nectar and nectary is maintained (for examples and previous literature, see Búrquez and Corbet, 1991; Nicolson, 1995; Langenberger and Davis, 2002; Stpiczynska, 2003*a*), apparently still promoted in *E. purpurea* by the nectar reservoir formed by the enlarged corolla base. In this study where insect pollinators were excluded and cross pollinations were not performed, a net reclamation of uncollected nectar continued throughout the PP2 and PP3 stages until eventual cessation in PP4. In future, it would be interesting to determine the fate of reabsorbed nectar-sugar molecules (Pedersen *et al*., 1958; Shuel, 1961; Stpiczynska, 2003*b*) in species of the the Asteraceae, including following an absence of pollination, to see whether any sugar can reappear in the nectar of florets of adjacent whorls within a capitulum.

In sunflower (*Helianthus annuus*), like *E. purpure*a, greatest nectar quantities occurred in pistillate-stage florets (Hadisoesilo and Furgala, 1986). However, maximum average volume (0·19 μL), nectar-solute concentration (61 %) and nectar-sugar quantity (157 μg) per disc floret of *E. purpurea* differed from *H. annuus*, in that nectar volumes and concentrations ranged from 0·71–1·13 μL and 36–57 %, respectively, among 18 cultivars, with up to 569 μg per pistillate-stage floret (Hadisoesilo and Furgala, 1986). In other studies of sunflower, however, mean nectar volumes and concentrations of 0·02–0·16 μL and 32–39 % (seven cultivars; Tepedino and Parker, 1982) and 0·04–0·32 μL and 26–70 % (47 lines; Vear *et al*., 1990) were comparable with those of *E. purpurea*.

Sucrose, fructose and glucose were detected in nectar of *E. purpurea* sampled from three phenological phases (SP, PP1 and PP2), although less of the former occurred at PP2. Hexoses are predominant over sucrose in most asteracean species (Percival, 1961; Galetto and Bernardello, 2003), although sucrose is occasionally even absent (Percival, 1961; Torres and Galetto, 2002). The combination of high solute concentration and mixture of hexoses with sucrose in the nectar of *E. purpurea* is common in a generalist pollination syndrome that involves bees, butterflies and moths (Baker and Baker, 1983; Cruden and Hermann, 1983; Galetto and Bernardello, 2003).

Nectary morphology

The floral nectary of *E. purpurea* is similar in morphology to that of many asteracean species, where the gland sits on top of the inferior ovary and surrounds the style base (Mani and Saravanan, 1999). By anthesis, spatial restrictions imposed by the adjacent floral organs of the disc floret had contributed to the final nectary shape and size in *E. purpurea*, as in other species (Davis *et al*., 1996). On its internal face, the circular outline of the nectary surface evidently reflected the nectary's expansion around a cylindrical style base, which was dilated above the floral nectary disk. The swollen style base immediately above the nectary in *Gochnatia polymorpha* (Sancho and Otegui, 2000), *Helianthus annuus* (Tacina, 1974), *Heterothalamus alienus* (Vogel, 1998) and *Tridax procumbens* (Gopinathan and Varatharajan, 1982), like that of *E. purpurea*, may result from constriction of the surrounding, expanding nectary around the narrowed, extreme base of the style.

Externally, the pentagonal outline suggests that the late-maturing floral nectary is partially molded during its expansion, against the five pre-formed, established petals of the corolla tube adjacent to it. Sammataro *et al*. (1985) reported that sunflower nectaries from many cultivars ranged from four- to eight-sided, and even circular, although it is unknown whether the number of nectary sides corresponded to the number of whorled floral parts adjacent to the nectary. Evidence of opposing external pressure applied by the surrounding corolla (fig. 1F) and even the filament bases (figs 2A and 3F in Sancho and Otegui, 2000), resulting in the undulating, pentagonal nature of the tall floral nectary of *G. polymorpha* (Sancho and Otegui, 2000), is also clear.

Floral nectaries of *E. purpurea* were slightly more than half the width and approx. 100 μm shorter than those of sunflower (Tacina, 1974; Sammataro *et al*., 1985). The internal diameter of sunflower floret nectaries varied from 470 to 800 μm and their heights varied from 200 to 360 μm (Sammataro *et al*., 1985). Diameters of the floral nectaries of *Wedelia chinensis* (440 μm) and *Tridax procumbens* (400 μm) (Gopinathan and Varatharajan, 1982) are also slightly larger than those of *E. purpurea*.

Nectary phloem

The floral nectary of *E. purpurea* was innervated directly and solely by phloem, consisting of sieve tubes that extended from the nectary base to about three-quarters of the height of the nectary. This occurrence of phloem alone within the nectary is in accordance with 27 % of Asteraceae studied previously (see Introduction). Although it is common for angiosperm nectaries to receive a direct vascular supply of phloem (Fahn, 1979), it is unusual to observe an intimate relationship between the phloem and epidermis. In the structureless nectaries on the outer perianth of *Paeonia*

albiflora (Paeoniaceae), Zimmermann (1932) drew phloem cells, beneath a guard cell, but these hypodermal elements of phloem did not match the length of the epidermal cells immediately above them. Interestingly, in the extranuptial nectaries of the involucral bracts of the capitulum of *Centaurea* spp., phloem also resides close to the epidermis and guard cells but is separated from them by a few cell layers of sclerenchyma (Zimmermann, 1932). This phenomenon of phloem in the hypodermis of floral nectaries in the Asteraceae has been demonstrated before in *Cirsium arvense*, *Helianthus tuberosus* (Frei, 1955) and *H. annuus* (Frei, 1955; Sammataro *et al*., 1985). Indeed, now in *E. purpurea* there is anatomical evidence for involvement of at least some epidermal cells in the ontogeny of sieve elements adjacent to them. Periclinal divisions of epidermal cells can result in the subepidermal precursors that yield the sieve tube element–companion cell complex. Moreover, within a sieve tube, the length of adjacent sieve elements varies and appears to depend on the size of the precursor cell itself. Furthermore, it appears that multiple, though diminutive, companion cells may form per sieve element.

Whereas the close proximity of the sieve tubes to the nectary surface strongly invokes phloem sap as a major contributor to nectar sugar in *E. purpurea*, and phloem exudates of the Asteraceae contain sucrose and some raffinose (Zimmermann and Ziegler, 1975), the demonstration of glucose and fructose in nectar of this species suggests that sucrose of phloem sap is not simply transported externally, but rather, sucrose inversion still occurs prior to ultimate secretion. If enzymes contributing to this modification of sucrose are only bound to cell walls rather than present in the nectar itself, it could be fruitful to explore regions of the epidermis near the sieve elements for localization and characterization of these catalysts.

The closeness of the sieve elements to the nectary epidermis of *E. purpurea* also probably allows an efficient retrieval system, for net reclamation of uncollected nectar carbohydrates. Recently, Masierowska and Stpiczynska (2005) detected radioactivity in sieve tubes following reabsorption of ^{14}C-labelled sucrose by the lateral nectaries of *Sinapis alba*, another species whose floral nectaries are supplied by phloem alone.

Cytologically, the sieve elements of the *E. purpurea* nectary share several features with those of other nectaries, including pore connections to adjacent elements at sieve plates (Durkee, 1983*a*), and various types of plastids, mitochondria and endoplasmic reticulum (Figier, 1971; Durkee, 1983*a*, *b*; Davis *et al*., 1988; Davis, 1992; Belmonte *et al*., 1994; Razem and Davis, 1999). As in *Echinacea*, sieve elements of nectary phloem can be connected by plasmodesmata to companion (Davis *et al*., 1988) and parenchyma (Sammataro *et al*., 1985; Davis *et al*., 1988) cells, and sieve elements may lie directly beside intercellular spaces (Sammataro *et al*., 1985; Davis, 1992; Razem and Davis, 1999).

The companion cells were particularly rich in mitochondria and ribosomes in the ground substance and stained densely, but with variability in intensity. In *E. purpurea*, companion cells were distinguished as the only units of the entire nectary modified as transfer cells (Pate and Gunning, 1972), their wall ingrowths enhancing the opportunity for active transport of pre-nectar constituents across the enlarged surface area of their cell membrane. In the floral nectary of *Helianthus annuus*, wall ingrowths were not reported by Sammataro *et al*. (1985), but Tacina (1979) identified wall protuberances in what might be a companion cell, if the unlabelled cell in the bottom right of his fig. 5 is a sieve element. Interestingly, companion cells involved in phloem loading at minor veins in leaves of *H. annuus*, are modified as transfer cells (Turgeon *et al*., 2001), but evidently this aspect is unknown for *Echinacea*. Other species with floral nectaries in the form of multicellular outgrowths that possess companion cells as their only transfer cells include *Eccremocarpus scaber* (Belmonte *et al*., 1994) and *Pisum sativum* (Razem and Davis, 1999). Floral nectaries of *E. purpurea* differ somewhat by having ingrowths along their walls opposite epidermal cells, but lacked ingrowths opposite the sieve elements. Otherwise, the companion cells of *E. purpurea* share with *Pisum sativum* (Razem and Davis, 1999) and *Vicia faba* (Davis *et al*., 1988) the orientation of wall ingrowths opposite other companion cells, phloem parenchyma and intercellular spaces. Accordingly, companion cells in *E. purpurea* may be instrumental in the unloading of phloem sap, arriving within the adjacent sieve elements, and passing pre-nectar constituents to the phloem parenchyma and intercellular spaces next to them.

The fibrillar substance found in phloem parenchyma cells (Fig. 6B) may be proteinaceous, sharing affinities with material identified in parenchyma adjacent to vascular tissue of floral and extrafloral nectaries (Durkee, 1983*a*; Belmonte *et al*., 1994) and elsewhere within the glands (Eymé, 1963; Baker *et al*., 1978; Schnepf and Deichgräber, 1984; Horner *et al*., 2003).

Parenchyma cells of the nectary

The presence of lobed nuclei lined by nuclear pores along cytoplasmic invaginations occurs in parenchyma (Zandonella, 1970*b*; Perrin and Zandonella, 1971) and in guard cells (Davis, 1992) of other floral nectaries and hydathodes, where it enables close contact between organelles with the nucleus and generally reflects a cell's heightened physiological activity (Perrin and Zandonella, 1971).

Plastids were common and possessed plastoglobuli but few thylakoids, in their stroma. Using oil immersion and light microscopy, plastids from unstained, fresh nectaries appeared yellowish, but it was impossible to ascertain whether the nectary's pale-yellow colour (Fig. 1B) was attributable only to chromoplasts, or included faintly pigmented vacuolar contents. In sectional profile, each plastid had one starch grain, or none. This paucity of starch in combination with the relative longevity (up to 4 d) of nectar secretion, in small quantities per floret, is generally indicative of floral nectaries dependent on other plant organs for their photosynthate throughout secretion (Pacini *et al*., 2003). The rich and direct supply of phloem to the nectary strongly favours phloem sap, supplemented to a lesser extent by plastid starch, as the principal source of nectar sugar. Some of the starch present might even originate from carbohydrate delivered by nectary phloem.

More starch per plastid was evident in pistillate-phase (Figs 7B and 8B) rather than staminate-phase (Fig. 7A) florets, and may serve as an intermediate reserve later in the secretory duration. However, it is also possible that some plastid starch is deposited during the net reabsorption process preceding cessation; plastid starch was highest in parenchyma of nectaries with fading petals than in the fully opened flower of red clover (Eriksson, 1977) and in post-secretory glands of *Cucurbita pepo* (Nepi *et al*., 1996). Plastids were often adjacent to mitochondria, sometimes closely wrapped around them, as in other nectaries (Zandonella, 1970*b*; Baker *et al*., 1978; Stpiczynska, 2003*a*).

Mitochondria were the most abundant macroorganelle in floral nectaries of *E. purpurea*, often existing in groups similar to those observed in other studies (Baker *et al*., 1978; Fahn and Benouaiche, 1979). Their omnipresence suggests that the mode of nectar secretion in *E. purpurea* is eccrine, dependent on energy for active transport of pre-nectar carbohydrates across cell membranes (Eriksson, 1977; Davis *et al*., 1986; Razem and Davis, 1999). However, a granulocrine secretory mechanism, dependent on reverse pinocytosis of vesicles to expel pre-nectar constituents from cell-to-cell and to the exterior, is less likely because endoplasmic reticulum remained a minor component of the cytoplasm compared with other nectaries (reviewed by Kronestedt-Robards and Robards, 1991). Dictyosomes, however, existed continually in both epidermal and subepidermal cells, and were also common in nectaries of sunflower (Tacina, 1979). Although their role may have been associated with cell-wall formation, involvement of dictyosomal vesicles in a granulocrine process cannot be totally excluded. Nectar formation in *E. purpurea* did not coincide with cellular disintegration of the nectary, and hence is not a holocrine process.

Complex vacuolar inclusions were detected in, or associated with, vacuoles of epidermal and parenchyma cells. In Fig. 8B, a constricted connection between a myelin-like multilamellar body and a multitubular body was evident, corroborating the finding of Eymé (1967) in floral nectaries of *Diplotaxis erucoides*, that these bodies are confluent. Eymé proposed that these inclusions originated near plasmodesmata from internalized trabeculae that form vesicles of membranes eventually residing in vacuoles, where they are a reserve of tonoplast membranes for new, interlocking vacuoles. In the cyathial nectary of *Euphorbia candelabrum*, Schnepf and Deichgräber (1984) indicated an involvement of endoplasmic reticulum in such bodies which myelinize in the centre. Eriksson (1977) found myelin figures in floral nectaries of *Trifolium pratense* before, during and after nectar secretion. Rather than serving as a source of new vacuoles (Eymé, 1967), in *E. purpurea* the authors propose that these types of inclusions have a lysosomal function, the bodies accumulating layers of membrane as they participate in a continual degradation of senescing organelles during nectary development and function. In certain cells of the pistillate phase of secretion, over 25 inclusions of a related nature were detected in a single cell profile (Fig. 8C). An enlarged vacuole and peripheral nucleus (Fig. 8C) have been associated with cell degradation in senescing nectaries (Zandonella, 1970*b*; Davis *et al*., 1986; Horner *et al*., 2003); apoptosis might even result. These types of inclusions have been reported in floral (Eymé, 1996, 1967; Zandonella, 1970*b*; Eriksson, 1977; Durkee *et al*., 1981; Davis *et al*., 1986) and extrafloral (Figier, 1971; Schnepf and Deichgräber, 1984; Freitas and Paoli, 1999) nectaries with regularity, such that it is difficult to dismiss them simply as artefactual, although much remains to be verified about their origin and role.

Features of modified stomata on the nectary surface

Evidently, very few modified stomata originate after the mature bud phase is reached, the overall average number (29·2) per gland being in close accord with *Cosmos bipinnatus* but exceeding three other species (Gopinathan and Varatharajan, 1982). Modified stomata occurred predominantly around the entire rim of the nectary of *E. purpurea* and were often raised as in *Helianthus annuus* (Sammataro *et al*., 1985), but only occurred sporadically on the sides of the gland. The latter commonly were immature and not raised above the epidermal cells, a pattern observed elsewhere (Webster *et al*., 1982; Davis and Gunning, 1992). The modified stomata were anomocytic, like those on other nectaries (Gopinathan and Varatharajan, 1982; Sancho and Otegui, 2000) and leaves (Sanchez, 1977) of the Asteraceae.

The stomata on the nectary surface of *E. purpurea* are considered 'modified' (Fahn, 1979) because they typically lack the ability to close their pores by guard-cell movements (Zandonella, 1967; Davis and Gunning, 1992, 1993). Movement is hindered because of contact maintained between guard cells and the secretory parenchyma below, resulting in a small substomatal space (Davis and Gunning, 1992, 1993; Gaffal *et al*., 1998; Razem and Davis, 1999), unlike foliar stomata of sunflower (Sanchez, 1977). The stomatal pores on the surface of asteracean nectaries remained open throughout day and night (Gopinathan and Varatharajan, 1982). Greatest average pore widths in *E. purpurea*, comparable with those of *Cosmos bipinnatus* and *Tridax procumbens* (Gopinathan and Varatharajan, 1982), occurred in the mature bud phase. This pattern is similar to the floral nectary of *Vicia faba* (Davis and Gunning, 1992), wherein the pore-width decrease associated with the onset of secretory activity may be related to wetting and turgor-pressure changes in guard cells (Davis and Gunning, 1992, 1993). Widths of the nectary stomata in *E. purpurea* were similar to those of two asteracean species studied by Galetto (1995).

Apart from mechanical constraints, the lack of synchrony between development of the modified stomata and nectar production also mitigates against a finely controlled regulation of nectar passage by the stomatal pores. Apertures were fully open—even widest—before secretion began, and immature stomata still occurred by the pistillate phase of nectar secretion, suggesting that some nectary stomata never reach maturity. However, it is known that not all open stomata participate as exits for nectar (Beardsell *et al*., 1989; Davis and Gunning, 1992; Gaffal *et al*.,

1998; Vezza *et al*., 2005). Also, direct microscopic observations are still required to determine whether nectar may yet pass through the developed pore of immature stomata, despite the intact, overlying outer cuticle that conceals the pore when viewed externally, by SEM.

Despite the restrictions on guard-cell movements that cause several open pores to persist, pores of the modified stomata on the floral nectaries of *E. purpurea* could become occluded by different means. Not reported previously in the Asteraceae (Gopinathan and Varatharajan, 1982), pore occlusion occurred like that in *Vicia faba* (Davis and Gunning, 1992) and *Pisum sativum* (Razem and Davis, 1999), throughout floret phenology but was greatest after nectar secretion commenced, and as florets aged. The nature of the occluding materials, and whether pore occlusion necessarily results in complete blockage of nectar flow, also requires investigation.

Pathway of pre-nectar to the nectary exterior

Ultrastructural evidence exists to support two commonly proposed routes of pre-nectar movement—the apoplastic and symplastic pathways—in the floral nectary of *E. purpurea*. The apoplastic route exists as a continuum of cell walls and intercellular spaces, the latter already formed prior to commencement of nectar secretion in the early staminate phase. Intercellular spaces abutting the sieve elements and companion cells of the nectary interior suggest that arriving phloem sap may already enter the apoplast at this step. The established continuity of intercellular spaces extending from the phloem to the substomatal chambers and pores of the modified stomata would facilitate pre-nectar transport and escape onto the nectary surface. Such an apoplastic route terminating at stomatal pores has been illustrated for several asteracean nectaries (Frei, 1955; Frey-Wyssling, 1955). An apoplastic pathway has been advocated for several non-trichomatous nectaries (Vassilyev, 1971; Gaffal *et al*., 1998; Durkee *et al*., 1999; Koteyava *et al*., 2005). In *E. purpurea*, an additional apoplastic pathway formed by gaps in the epidermis, exists at a limited number of creases (Figs 2B and 4E) that apparently circumvents the epidermal cells altogether. Epidermal gaps in nectaries are reported elsewhere (Vogel, 1998), but in *Vicia faba* are apical, non-stomatal openings adjacent to guard cells (Davis and Gunning, 1993), unlike *E. purpurea*.

A symplastic route dependent on intercellular plasmodesmatal connections is also available in the floral nectary of *E. purpurea*, from the phloem to the epidermis. Plasmodesmata connect sieve elements to companion and phloem-parenchyma cells, and these in turn have plasmodesmatal connections to parenchyma and epidermal cells. A continuous symplastic path to the epidermis requires an apoplastic step across the anticlinal or outer periclinal wall to the nectary surface. This transfer to the exterior may be facilitated by microchannels in the cuticle (Fig. 5D) lining the outer nectary surface, similar to other nectaries (Radice and Galati, 2003).

In many nectaries, ultrastructural evidence has demonstrated that both apoplastic and symplastic routes for pre-nectar transport and escape are feasible (Davis *et al*., 1986, 1988; Kronestedt and Robards, 1987; Nichol and Hall, 1988; Razem and Davis, 1999), and it is concluded that carbohydrate arriving in the nectary phloem of *E. purpurea* may simultaneously be transferred to the nectary exterior by a combination of these routes.

ACKNOWLEDGEMENTS

We thank Mrs Sarah Caldwell and Dr L. C. Fowke for their guidance and assistance with the TEM; Dr B. Barl for donation of plants; Mr Dennis Dyck for assistance with preparation of electronic versions of the TEM plates; and Mr Daryn Bikey and Dr N. H. Low for conducting the HPLC analyses of *E. purpurea* nectar; and two anonymous reviewers for their helpful comments. Funding to T.J.W. in the form of a Graduate Scholarship from the University of Saskatchewan, and to the project (A.R.D.) from the Agri-Food Innovation Fund and a Discovery Grant from NSERC of Canada, is gratefully acknowledged.

LITERATURE CITED

Baker DA, Hall JL, Thorpe JR. 1978. A study of the extrafloral nectaries of *Ricinus communis*. *New Phytologist* **81**: 129–137.

Baker HG, Baker I. 1983. A brief historical review of the chemistry of floral nectar. In: Bentley B, Thomas E, eds. *The biology of nectaries*. New York, NY: Columbia University Press, 126–152.

Bauer R. 1998. The Echinacea story—the scientific development of an herbal immunostimulant. In: Prendergast HDV, Etkin NL, Harris DR, Houghton PJ, eds. *Plants for food and medicine*. London: Royal Botanic Gardens Kew, 317–332.

Beardsell DV, Williams EG, Knox RB. 1989. The structure and histochemistry of the nectary and anther secretory tissue of the flowers of *Thryptomene calycina* (Lindl.) Stapf. (Myrtaceae). *Australian Journal of Botany* **37**: 65–80.

Belmonte E, Cardemil L, Kalin Arroyo MT. 1994. Floral nectary structure and nectar composition in *Eccremocarpus scaber* (Bignoniaceae), a hummingbird-pollinated plant of central Chile. *American Journal of Botany* **81**: 493–503.

Bonnier G. 1879. Les nectaires—étude critique, anatomique et physiologique. *Annales de Sciences Naturelles Botanique* **8**: 5–212.

Búrquez A, Corbet SA. 1991. Do flowers reabsorb nectar? *Functional Ecology* **6**: 369–379.

Caspary JXR. 1848. *De Nectariis. Commentationem botanicuam conscripsit*. Kayser Bucher Lexikon 11/12: 84.

Crane E. 1975. *Honey: a comprehensive survey*. London: William Heinemann.

Cruden RW, Hermann SM. 1983. Studying nectar? Some observations on the art. In: Bentley B, Thomas E, eds. *The biology of nectaries*. New York, NY: Columbia University Press, 223–241.

Davis AR. 1992. *Physiological and structural aspects of floral nectar secretion*. PhD Thesis, Australian National University, Canberra.

Davis AR, Gunning BES. 1992. The modified stomata of the floral nectary of *Vicia faba* L. 1. Development, anatomy and ultrastructure. *Protoplasma* **166**: 134–152.

Davis AR, Gunning BES. 1993. The modified stomata of the floral nectary of *Vicia faba* L. 3. Physiological aspects, including comparisons with foliar stomata. *Botanica Acta* **106**: 241–253.

Davis AR, Peterson RL, Shuel RW. 1986. Anatomy and vasculature of the floral nectaries of *Brassica napus* (Brassicaceae). *Canadian Journal of Botany* **64**: 2508–2516.

Davis AR, Peterson RL, Shuel RW. 1988. Vasculature and ultrastructure of the floral and stipular nectaries of *Vicia faba* (Leguminosae). *Canadian Journal of Botany* **66**: 1435–1448.

Davis AR, Fowke LC, Sawhney VK, Low NH. 1996. Floral nectar secretion and ploidy in *Brassica rapa* and *Brassica napus* (Brassicaceae). II.

Quantified variability of nectary structure and function in rapid-cycling lines. *Annals of Botany* **77**: 223–234.

Davis AR, Pylatuik JD, Paradis JC, Low NH. 1998. Nectar-carbohydrate production and composition vary in relation to nectary anatomy and location within individual flowers of several species of Brassicaceae. *Planta* **205**: 305–318.

Durkee LT. 1983*a*. Protein-containing cells in the nectary phloem of *Passiflora warmingii*. *American Journal of Botany* **70**: 1011–1018.

Durkee LT. 1983*b*. Ultrastructure of nectaries. In: Bentley B, Thomas E. eds. *The biology of nectaries*. New York, NY: Columbia University Press, 1–29.

Durkee LT, Gaal DJ, Reisner WH. 1981. The floral and extra-floral nectaries of *Passiflora*. I. The floral nectary. *American Journal of Botany* **68**: 453–462.

Durkee LT, Haber MH, Dorn L, Remington A. 1999. Morphology, ultrastructure, and function of extrafloral nectaries in three species of Caesalpiniaceae. *Journal of the Iowa Academy of Science* **106**: 82–88.

Eriksson M. 1977. The ultrastructure of the nectary of red clover (*Trifolium pratense*). *Journal of Apicultural Research* **16**: 184–193.

Eymé J. 1963. Observations cytologiques sur les nectaires de trois Renonculacées (*Helleborus foetidus* L., *H. niger* L. et *Nigella damascena* L.). *Le Botaniste* **46**: 137–179.

Eymé J. 1966. Infrastructure des cellules nectarigènes de *Diplotaxis erucoides* D.C., *Helleborus niger* L. et *H. foetidus* L. *Comptes rendus hebdomadaires des séances de l'Académie des sciences. Série D, Sciences naturelles* **262**: 1629–1632.

Eymé J. 1967. Nouvelles observations sur l'infrastructure de tissus nectarigènes floraux. *Le Botaniste* **50**: 169–183.

Fahn A. 1979. *Secretory tissues in plants*. New York, NY: Academic Press.

Fahn A, Benouaiche P. 1979. Ultrastructure, development and secretion in the nectary of banana flowers. *Annals of Botany* **44**: 85–93.

Figier J. 1971. Étude infrastructurale de la stipule de *Vicia faba* L. au niveau du nectaire. *Planta* **98**: 31–49.

Frei E. 1955. Die Innervierung der floralen Nektarien dikotyler Pflanzenfamilien. *Berichte der Schweizerischen Botanischen Gesellschaft* **65**: 60–114.

Freitas L, Paoli AAS. 1999. Structure and ultrastructure of the extrafloral nectaries of *Croton urucurana* Baill. (Euphorbiaceae). *Boletim de Botanica de Universidade São Paolo* **18**: 1–10.

Frey-Wyssling A. 1955. The phloem supply to the nectaries. *Acta Botanica Neerlandica* **4**: 358–369.

Gaffal KP, Heimler W, El-Gammal S. 1998. The floral nectary of *Digitalis purpurea* L., structure and nectar secretion. *Annals of Botany* **81**: 251–262.

Galetto L. 1995. Estudios sobre el nectar y los nectaries en *Hyaloseris rubicunda* y *Barnadesia odorata* (Asteraceae-Mutisieae). *Darwiniana* **33**: 127–133.

Galetto L, Bernardello G. 2003. Nectar sugar composition in angiosperms from Chaco and Patagonia (Argentina): an animal visitor's matter? *Plant Systematics and Evolution* **238**: 69–86.

Gopinathan K, Varatharajan R. 1982. On the morphology, topography and the significance of stomata on floral nectaries of some Compositae. *Phytomorphology* **32**: 265–269.

Gulyás S, Pesti J. 1966. Angaben zur Anatomie der Nektarien der Centaureae. *Acta Biologica Szeged* **12**: 17–23.

Gunning BES, Pate JS. 1969. Transfer cells: plant cells with wall ingrowths, specialized in relation to short distance transport of solutes – their occurrence, structure, and development. *Protoplasma* **68**: 107–133.

Hadisoesilo S, Furgala B. 1986. The effect of cultivar, floral stage and time of day on the quantity and quality of nectar extracted from oilseed sunflower (*Helianthus annuus* L.) in Minnesota. *American Bee Journal* **122**: 648–652.

Horner HT, Healy RA, Cervantes-Martinez T, Palmer RG. 2003. Floral nectary fine structure and development in *Glycine max* L. (Fabaceae). *International Journal of Plant Science* **164**:675–690.

Kartashova NN. 1965. *Stroeniei funcktsiya nektarnikov tsvetkadvudol'nykh rastenii*. Istadel'stvo Tomskogo Universiteta, Tomsk.

Kindscher K. 1989. Ethnobotany of purple coneflower (*Echinacea angustifolia*, Asteraceae) and other *Echinacea* species. *Economic Botany* **43**: 498–507.

Koteyava NK, Vassilyev AE, Tarlyn N, Franceschi VR. 2005. On mechanisms of nectar secretion. Abstract 10.3.4, XVII International Botanical Congress, Vienna, Austria, p. 162.

Kronestedt EC, Robards AW. 1987. Sugar secretion from the nectary of *Strelitzia*: an ultrastructural and physiological study. *Protoplasma* **137**: 168–182.

Kronestedt-Robards EC, Robards AW. 1991. Exocytosis in gland cells. In: Hawes CR, Coleman JOD, Evans DE, eds. *Endocytosis, exocytosis and vesicle traffic in plants*. Cambridge: Cambridge University Press, 199–232.

Langenberger MW, Davis AR. 2002. Temporal changes in floral nectar production, reabsorption, and composition associated with dichogamy in annual caraway (*Carum carvi*; Apiaceae). *American Journal of Botany* **89**: 1588–1598.

McGregor RL. 1968. The taxonomy of the genus *Echinacea* (Compositae). *University of Kansas Science Bulletin* **48**: 113–142.

McKenna M, Thomson JD. 1988. A technique for sampling and measuring small amounts of floral nectar. *Ecology* **69**: 1036–1037.

Ma H, Xiao AJ, Cao R. 2002. Developmental and anatomic studies on the floral nectaries of *Tugarinovia mongolica*. *Acta Botanica Yunnanica* **24**: 638–644.

Mani MS, Saravanan JM. 1999. *Pollination ecology and evolution in Compositae (Asteraceae)*. Enfield, NH, USA: Science Publishers Inc.

Masierowska ML, Stpiczynska M. 2005. Nectar resorption in flowers of *Sinapis alba* L., Brassicaceae and *Platanthera chlorantha* Custer (Rchb.), Orchidaceae. Abstract PO383. XVII International Botanical Congress, Vienna, Austria, p. 300.

Nepi M, Ciampolini F, Pacini E. 1996. Development and ultrastructure of *Cucurbita pepo* nectaries of male flowers. *Annals of Botany* **78**:95–104.

Nichol P, Hall JL. 1988. Characteristics of nectar secretion by the extrafloral nectaries of *Ricinus communis*. *Journal of Experimental Botany* **39**: 573–586.

Nicolson SW. 1995. Direct demonstration of nectar reabsorption in the flowers of *Grevillea robusta* (Proteaceae). *Functional Ecology* **9**: 584–588.

Pacini E. 1996. Tapetum types in the Compositae: forms and function. In: Hind DJN, Beentje HJ, eds. *Proceedings of the International Compositae Conference*, Royal Botanic Gardens, Kew, 21–28.

Pacini E, Nepi M, Vesprini JL. 2003. Nectar biodiversity: a short review. *Plant Systematics and Evolution* **238**: 7–21.

Pate JS, Gunning BES. 1972. Transfer cells. *Annual Review of Plant Physiology* **23**: 173–196.

Pederson MW, Lefevre CW, Wiebe HH. 1958. Absorption of C^{14} labelled sucrose by alfalfa nectaries. *Science* **127**: 758–759.

Percival MS. 1961. Types of nectar in angiosperms. *New Phytologist* **60**: 235–281.

Perrin A, Zandonella P. 1971. Presence d'invagination nucleaires dans les cellules de quelques nectaires floraux et hydathodes. *Planta* **96**: 136–144.

Proctor M, Yeo P, Lack A. 1996. *The natural history of pollination*. London: Collins New Naturalist.

Radice S, Galati BG. 2003. Floral nectary ultrastructure of *Prunus persica* (L.) Batch cv. Forastero (Newcomer), an Argentine peach. *Plant Systematics and Evolution* **238**: 23–32.

Razem FA, Davis AR. 1999. Anatomical and ultrastructural changes of the floral nectary of *Pisum sativum* L. during flower development. *Protoplasma* **206**: 57–72.

Reynolds ES. 1963. The use of lead citrate at high pH as an electron-opaque stain in electron microscopy. *Journal of Cell Biology* **17**: 208–212.

Sammataro D, Erickson EH, Garment MB. 1985. Ultrastructure of the sunflower nectary. *Journal of Apicultural Research* **24**: 150–160.

Sanchez SM. 1977. The fine structure of the guard cells of *Helianthus annuus*. *American Journal of Botany* **64**: 814–824.

Sancho G, Otegui M. 2000. Vascularization and secretory tissues in florets of *Gochnatia polymorpha* (Asteraceae, Mutisieae): evolutionary considerations. *Phytomorphology* **50**: 172–179.

Schnepf E, Deichgräber G. 1984. Electron microscopical studies of nectaries of some *Euphorbia* species. *Akademie der Wissenschaften und der Literatur, Mainz. Tropische und subtropische Pflanzenwelt* **45**: 55–93.

Shuel RW. 1961. Influence of reproductive organs on secretion of sugars in flowers of *Streptosolen jamesonii* Miers. *Plant Physiology* **36**: 265–271.

Shuel RW. 1992. The production of nectar and pollen. In: Graham JM, ed. *The hive and the honey bee*. Hamilton, IL: Dadant, 401–436.

Stpiczynska M. 2003*a*. Nectar reabsorption in the spur of *Platanthera chlorantha* Custer (Rchb.) Orchidaceae: structural and micro-autoradiographic study. *Plant Systematics and Evolution* **238**: 119–126.

Stpiczynska M. 2003*b*. Incorporation of (^{3}H) sucrose after the reabsorption of nectar from the spur of *Platanthera chlorantha* (Custer) Rchb. *Canadian Journal of Botany* **81**: 927–932.

Tacina F. 1974. Observatii morfoanatomice comparative asupra glandelor nectarifere de la unele soiuri de floarea-soarelui. *Studii si Cercet Ari de Biologie* **26**: 3–7.

Tacina F. 1979. Corelatia dintre ultrastructura celulelor nectarifere si secretia de nectar la floarea-soarelui. *Apicultura in Romania* **54**: 15–19.

Tepedino VJ, Parker FD. 1982. Interspecific differences in the relative importance of pollen and nectar to bee species foraging on sunflowers. *Environmental Entomology* **11**: 246–250.

Torres C, Galetto L. 2002. Are nectar sugar composition and corolla tube length related to the diversity of insects that visit Asteraceae flowers? *Plant Biology* **4**: 360–366.

Turgeon R, Medville R, Nixon KC. 2001. The evolution of minor vein phloem and phloem loading. *American Journal of Botany* **88**: 1331–1339.

Vassilyev AE. 1971. New data on the ultrastructure of the cells of the flower nectary. *Akad Nauk SSSR Botanical Journal* **56**: 1292–1306 [in Russian with English summary].

Vear F, Pham-Delegue M, Tourvielle de Labrouhe D, Marileau R, Loublier Y, le Métayer M, *et al*. 1990. Genetical studies of nectar and pollen production in sunflower. *Agronomie* **10**: 219–231.

Vezza M, Nepi M, Guarnieri M, Artese D, Rascio N, Pacini E. 2006. Ivy (*Hedera helix*) flower nectar and nectary ecophysiology. *International Journal of Plant Sciences* (in press).

Vogel S. 1998. Remarkable nectaries: structure, ecology, organophyletic perspectives. IV. Miscellaneous cases. *Flora* **193**: 225–248.

Wagner H. 1999. Phytomedicine in Germany. *Environmental Health Perspectives* **10**: 779–781.

Warakomska Z, Kolasa Z. 2003. The flowering biology and apicultural value of coltsfoot (*Tussilago farfara* L.f. Asteraceae). *Annals Universitatis Mariae Curie – Sklodowska* **58**: 1–8.

Webster BD, Ross DM, Evans T. 1982. Nectar and the nectary of *Phaseolus vulgaris*. *Journal of the American Society for Horticultural Science* **107**: 497–503.

Zandonella P. 1967. Stomates des nectaires floraux chez les Centrospermales. *Bulletin Societé Botanique du France* **114**: 11–20.

Zandonella P. 1970*a*. Infrastructure des cellules du tissu nectarigène floral de quelques Caryophyllaceae. *Comptes rendus hebdomadaires des séances de l'Académie des sciences. Série D, Sciences naturelles* **270**: 1310–1313.

Zandonella P. 1970*b*. Infrastructure du tissu nectarigène floral de *Beta vulgaris* L.: le vacuome et la dégradation du cytoplasme dans les vacuoles. *Comptes rendus hebdomadaires des Séances de l'Académie des sciences. Série D, Sciences naturelles* **271**: 70–73.

Zimmermann JG. 1932. Über die extrafloralen Nektarien der Angiospermen. *Beihefte zum Botanischen Centralblatt* **49**: 99–196.

Zimmermann MH, Ziegler H. 1975. List of sugars and sugar alcohols in sieve-tube exudates. In: Zimmermann MH, Milburn JA, eds. *Encyclopedia of plant physiology: transport in plants.* I. *Phloem transport*. New York, NY: Springer, 480–503.